UNIVERSIDAD DE CONCEPCIÓN

Centro de Investigación en Ingeniería Matemática (CI^{2}MA)

Centrifugal settling of flocculated suspensions: A sensitivity analysis of parametric model functions

Stefan Berres, Raimund Bürger,
Rodrigo Garces

PREPRINT 2010-01

SERIE DE PRE-PUBLICACIONES

Centrifugal settling of flocculated suspensions: A sensitivity analysis of parametric model functions

Stefan Berres[1], Raimund Bürger[2,*] and Rodrigo Garcés[3]

[1]Departamento de Ciencias Matemáticas y Físicas, Facultad de Ingeniería, Universidad Católica de Temuco, Temuco, Chile.
E-Mail: sberres@uct.cl

[2]CI²MA and Departamento de Ingeniería Matemática, Facultad de Ciencias Físicas y Matemáticas, Universidad de Concepción, Casilla 160-C, Concepción, Chile.
E-mail: rburger@ing-mat.udec.cl

[3]Departamento de Ingeniería Matemática, Facultad de Ingeniería, Ciencias y Administración, Universidad de La Frontera, Temuco, Chile,
E-Mail: rgarc008@pinhue.ufro.cl

Abstract

The centrifugal settling of a flocculated suspension in a rotating tube can be modelled by a strongly degenerate parabolic partial differential equation whose coefficients depend on two material-specific model functions, namely the hindered settling function and the effective solid stress function. These model functions are usually given by certain nonlinear algebraic expressions that involve a small number of parameters. The present work is related to the problem of determining these parameters for a given material. This problem of parameter identification consists in minimizing the distance between observed and simulated concentration profiles by successively varying the parameters employed for the simulation, starting from an initial guess. The feasibility and robustness of this procedure, which does not necessarily lead to a unique solution, decisively depends on the sensitivity of the solution of the direct problem to the different scalar parameters. These sensitivities are evaluated by a series of numerical experiments. It turns out that the model is extremely sensitive to the choice of the so-called critical concentration marking the transition between hindered settling and compression. Moreover, the robustness of the parameter identification method depends significantly on

[*] Corresponding author.

whether intermediate (i.e., transient) or stationary concentration profiles are used for identification.

Keywords

Centrifugation, Numerical Simulation, Sedimentation, Flocculated Suspension, Parameter Identification, Sensitivity Analysis

1 Introduction

1.1 Scope

The settling of a monodisperse flocculated suspension in a rotating tube centrifuge can be modelled by the following spatially one-dimensional strongly degenerate parabolic-hyperbolic partial differential equation (PDE) for the local solids concentration (volume fraction) $\phi = \phi(r,t)$ as a function of radial position r and time t [1–3]:

$$\frac{\partial \phi}{\partial t} + \frac{\partial}{\partial r}\left(-\frac{\omega^2 r}{g} f(\phi) \right) = \frac{\partial^2 A(\phi)}{\partial r^2}, \tag{1}$$

where ω is the angular velocity, g is the acceleration of gravity, the batch hindered settling function $f(\phi)$ is the first of two material-specific model functions of the local solids concentration ϕ, and the integrated diffusion function $A(\phi)$ is given by

$$A(\phi) := \int_0^{\phi} a(s)\mathrm{d}s,$$

where we define the diffusion coefficient

$$a(\phi) := -\frac{f(\phi)\sigma_{\mathrm{e}}'(\phi)}{\Delta\rho g \phi}, \qquad \sigma_{\mathrm{e}}'(\phi) := \frac{\mathrm{d}\sigma_{\mathrm{e}}(\phi)}{\mathrm{d}\phi}.$$

Here, $\Delta\rho > 0$ is the solid-fluid density difference and $\sigma_{\mathrm{e}}'(\phi)$ is the derivative of the second material-specific model function, namely the effective solids stress function $\sigma_{\mathrm{e}}(\phi)$.

Equation (1), together with suitable initial and boundary conditions that are given below, can be discretized by a fully implicit first-order finite difference scheme to allow the efficient simulation of the settling process. This requires, of course, that the functions $f(\phi)$ and $\sigma_{\mathrm{e}}(\phi)$ be given for the material under consideration.

The model employed herein is based on the assumption that there exists a critical concentration (or gel point) denoted by ϕ_{c}, such that wherever $\phi = \phi(r,t) < \phi_{\mathrm{c}}$, there is no contact between the particles, while for $\phi = \phi(r,t) \geq \phi_{\mathrm{c}}$, the particles form a compressible sediment layer. This means that

$$\sigma_{\mathrm{e}}'(\phi) \begin{cases} = 0 & \text{for } \phi \leq \phi_{\mathrm{c}}, \\ > 0 & \text{for } \phi > \phi_{\mathrm{c}}. \end{cases}$$

For details on the underlying sedimentation-consolidation theory we refer to Berres et al. [4] In mathematical terms, we obtain that the governing PDE (1) is of second-order parabolic type for $\phi > \phi_c$. For $\phi < \phi_c$, (1) degenerates into the first-order hyperbolic equation of a known kinematic centrifugation model that has been employed by several authors.[5–9] The basic problem is that the location of the type-change interface $\phi = \phi_c$, corresponding to the sediment level, is not known a priori and is part of the solution.

The present contribution addresses the problem of identifying certain material specific parameters that define the functions $f(\phi)$ and $\sigma_e(\phi)$ from measured concentration profiles. In what follows, we will refer to concentration profiles that have been obtained from measurements and, alternatively, by the (numerical) solution of the mathematical model for a given choice of these parameters, as *observed* and *simulated* data, respectively. The inverse problem of parameter identification consists in varying the (unknown) parameters until the best approximation of the observation by the simulation is attained. The degree of approximation, that is, the distance between observed and simulated data, is defined by a suitable *cost function*. Consequently, the problem of parameter identification can be regarded as the optimization problem of minimizing this cost function. The variation of parameters is done herein by a Quasi-Newton method. Sensitivity indicators like the condition number of the Hessian matrix of the cost function in its minimum are calculated.

In the present model one can distinguish three different types of parameters: the so-called "parabolic" parameters appear in the function $\sigma_e(\phi)$ and therefore affect only the (degenerating) diffusion function; the "hyperbolic" parameters are those of the function $f(\phi)$ and appear in both the convective and diffusive terms; and the critical concentration ϕ_c as a "hyperbolic-parabolic switch" parameter that controls whether the diffusion function is active, i.e., the mixture is subject to sediment compressibility at (r,t).

The number of identifiable parameters is ususally restricted by the quantity of information in the observation. For example, if there is only one single datum of information (e.g., the speed of the supernatant-suspension interface at one given time) which corresponds to the flux function, then only one parameter in $f(\phi)$ can be identified, since there is only one equation to solve. For a given non-linear parametric form, some parameters are supposed to have a stronger independent influence on the solution structure, whereas other parameters are more correlated. One goal of this study is to identify different degrees of independence of parameters in our sedimentation-consolidation model. Therefore, the influence of various parameter subsets is compared. One central goal is to decide which parameters have the strongest correlation and exclude them from the set of parameters to identify. The goal is to obtain an appropriate parameter set, where the parameters are meaningful in the sense that they show only small correlations with each other.

1.2 Related work

To put this work further into the proper perspective, let us first mention that related theoretical models, in part for polydisperse suspensions and including filter media, are presented by Berres et al.[2], Biesheuvel et al. [10], Biesheuvel and Verweij[11] , Sambuichi et al.[12] , Demeler et al. [13] and Stickland et al. [14]. On the other hand, it is well known that one-dimensional models such as Eq. (1) do not represent an adequate approximate description of the sedimentation of a rotating mixture in general; among the restrictions under which Eq. (1) is acceptable, the angular velocity ω must be large enough so that gravity is negligible but small enough so that Coriolis effects are unimportant.[1, 6] A survey on models for the centrifugal separation of a mixture is given by Schaflinger [15] (see also Stibi and Schaflinger [16]). However, there is a fairly large number of combined theoretical and experimental studies that confirm that one-dimensional models such as Eq. (1), or its slightly more involved version for rotating basket centrifuges,

$$\frac{\partial \phi}{\partial t}+\frac{1}{r}\frac{\partial}{\partial r}\left(-\frac{\omega^2 r^2}{g}f(\phi)\right)=\frac{1}{r}\frac{\partial}{\partial r}\left(r\frac{\partial A(\phi)}{\partial r}\right),$$

provide at least a useful approximation for laboratory-scale centrifuges, see Detloff and Lerche[7], Lerche and Frömer[8] , Chu and Lee[17, 18], Detloff et al. [19, 20], Eckert et al. [21], Frömer and Lerche[22], Hwang and Chou[23], Lerche[24] and Sambuichi et al. [25] (this list is not complete). Most of these papers present experimental data to which the parameter identification technique presented herein could be applied.

Berres et al. [26, 27] solved the parameter identification problem for the centrifugation model (1) numerically by an adjoint method. It turned out that when the method is applied to synthetic observations generated by a numerical scheme for (1) with given parameters (a problem known as *parameter recognition*), then only some of the identified parameter values are close to the values originally used for the simulation, while others remain close to their initial guess. (See, for example, Tables 1 and 2 in Berres et al. [26]) It is this observation of different sensitivities of different parameters which has motivated the present paper.

Finally, we mention that related problems of parameter identification in the context of applications to drying problems include the papers by Kada and Tarasiewicz [28] and Weres et al.[29]

2. Methods

2.1 Initial and boundary conditions; parametric forms of the model functions

The mathematical model describes the evolution of the concentration $\phi = \phi(r,t)$ with respect to time *t* and position *r*, where *t* takes values in the interval $0 \le t \le T$ and *r* varies between the inner and outer radii of the centrifuge, R_1 and R_2, respectively, i.e., $R_1 \le r \le R_2$. The evolution of $\phi = \phi(r,t)$ is described by Eq. (1), where it is assumed that the initial condition (at time $t = 0$) is given by $\phi(r,0) = \phi_0(r) = \phi_0$, which corresponds to an initially homogenous mixture of constant concentration ϕ_0. At the boundaries the centrifuge is closed, which gives rise to the zero-flux boundary condition

$$\left(\frac{\omega^2 r_b}{g} f(\phi) + \frac{\partial A(\phi)}{\partial r} \right)(r_b, t) = 0 \quad \text{at } r_b = R_1 \text{ and } r_b = R_2.$$

A common parametric form for the flux function $f(\phi)$ is due to Richardson and Zaki: [30]

$$f(\phi) = \begin{cases} v_\infty \ \phi(1-\phi)^C & \text{for } 0 \le \phi \le 1, \\ 0 & \text{otherwise,} \end{cases}$$

with the parameters $v_\infty < 0$, corresponding to the settling velocity of a single particle in an unbounded fluid, and the Richardson-Zaki exponent $C > 1$. A typical expression for the effective solid stress function $\sigma_e(\phi)$ is given by the power law [31]

$$\sigma_e(\phi) = \begin{cases} \sigma_0 \left[(\phi/\phi_c)^k - 1 \right] & \text{for } \phi > \phi_c, \\ 0 & \text{otherwise} \end{cases}$$

with parameters $k > 0$, $\sigma_0 \ge 0$ and $0 < \phi_c \le 1$.

2.2 Disretization of the direct problem

We first describe the numerical method to solve the initial-boundary value problem for (1) that describes the centrifugal settling process. The space-time domain is discretized by a grid with spatial cells of width $\Delta r = (R_2 - R_1)/M$, where M is an integer, and a time step $\Delta t = T/N$ such that there are points $r_j = R_1 + j\Delta r$, $t_n = n\Delta t$, $j = 0,\dots,M$, $n = 1,\dots,N$, for which the approximation $\phi_j^n \approx \phi(r_j, t_n)$ is computed, starting from $\phi_j^0 = \phi_0$. The "interior" marching formula has the form

$$\begin{aligned} &\frac{\phi_j^{n+1} - \phi_j^n}{\Delta t} - \frac{\omega^2}{\Delta r}\left(r_{j+1/2} f_{j+1/2}^{n+1} - r_{j-1/2} f_{j-1/2}^{n+1}\right) \\ &= \frac{A(\phi_{j+1}^{n+1}) - 2A(\phi_j^{n+1}) + A(\phi_{j-1}^{n+1})}{(\Delta r)^2}, \\ &j = 1,2,\dots,M-1,\ n = 0,1,2,\dots,N-1, \end{aligned} \tag{2}$$

where we define the numerical flux

$$f_{j+1/2}^{n+1} = f^{\mathrm{EO}}\left(u_j^{n+1}, u_{j+1}^{n+1}\right),$$

where f^{EO} denotes the Engquist-Osher[32] flux given by

$$f^{\mathrm{EO}}(u,v) := f(0) + \int_0^u \max\{0, f'(s)\}\,\mathrm{d}s + \int_0^v \min\{0, f'(s)\}\,\mathrm{d}s.$$

For $j = 0$ and $j = M$ we employ the following "boundary schemes", which result from modifying (2) by discrete versions of the zero-flux boundary conditions:

$$\frac{\phi_0^{n+1} - \phi_0^n}{\Delta t} - \frac{\omega^2}{\Delta r} r_{1/2} f_{1/2}^{n+1} = \frac{A(\phi_1^{n+1}) - A(\phi_0^{n+1})}{(\Delta r)^2} \tag{3}$$

and

$$\frac{\phi_M^{n+1} - \phi_M^n}{\Delta t} + \frac{\omega^2}{\Delta r} r_{M-1/2} f_{M-1/2}^{n+1} = \frac{A(\phi_{M-1}^{n+1}) - A(\phi_M^{n+1})}{(\Delta r)^2}. \tag{4}$$

The numerical scheme defined by Eqs. (2)–(4) represents a system of nonlinear equations, which are solved iteratively in each time step by the Newton-Raphson method. The basic advantage of the implicit discretization lies in the fact that no limitation on the size of time step Δt needs to be imposed, i.e., the scheme is always stable. Finally, we mention that numerical simulations of centrifugal separation obtained by the explicit version of (2)–(4) are presented by Bürger and Concha[1] and Garrido et al. [3]

According to one of the examples by Bürger and Concha[1], we herein use the parameters $R_1 = 0,06$ m, $R_2 = 0,3$ m, $\omega^2 = 327,000$ (rad/s)^2 (such that $R_2\omega^2 = 10000g$, where $g = 9.81$ m/s^2), $\Delta\rho = 1660$ kg/m^3, $v_\infty = -0,0001$ m/s, $M = 50$, $N = 6000$, $\phi_0 = 0,07$, and $h = 6,0555e-6$ and the tolerance of the gradient of the cost function $g_{\mathrm{tol}} = 1e-8$ (see Sect. 3).

2.3 Inverse problem

The task of the inverse problem is to determine parameters such that the cost function that measures the distance between the model solution and the observation is minimized. The cost function is calculated as distance between the observation profile $\hat{\phi}(r,t)$ and the solution $\phi(r,t)$

$$J = \int_0^L \left(\phi(r,t) - \hat{\phi}(r,t)\right)^2 \mathrm{d}r$$

for a fixed time t. In the examples this fixed time is set to $t = 0.1$ s and $t = 1.2$ s for the intermediate and stationary observation profile, respectively. Using a discrete approximation of the solution ϕ_j^n, we approximate the cost function by

$$\sum_{j=1}^{M} \left(\phi_j^n - \hat{\phi}_j^n\right)^2, \text{ where } \hat{\phi}_j^n = \hat{\phi}(j\Delta r, t^n).$$

The optimization algorithm approximates the optimal solution iteratively. Given the parameter vector of, say, four parameters,

$$p^{(n)} = \left(p_1^{(n)}, p_2^{(n)}, p_3^{(n)}, p_4^{(n)}\right),$$

at step *n* of the optimization procedure ($n = 1,2,3,\ldots$), the next (improved) parameter vector is calculated as

$$p^{(n+1)} = p^{(n)} - \alpha^{(n)} d^{(n)},$$

where $\alpha^{(n)}$ is a scalar variable for the one-dimensional line-search. The direction vector $d^{(n)}$ has for a Quasi-Newton method the form

$$d^{(n)} = H_{(n)}^{-1} \nabla J\left(p^{(n)}\right),$$

where $H_{(n)}^{-1}$ is an approximation of the inverse of the Hessian matrix of the cost function. The Hessian matrix for four parameters is defined as

$$H(p)=\left(\frac{\partial^2 J(p)}{\partial p_j \partial p_k}\right)_{(j,k=1,\ldots,4)}=\begin{pmatrix} \frac{\partial^2 J(p)}{\partial p_1^2} & \frac{\partial^2 J(p)}{\partial p_1 \partial p_2} & \frac{\partial^2 J(p)}{\partial p_1 \partial p_3} & \frac{\partial^2 J(p)}{\partial p_1 \partial p_4} \\ \frac{\partial^2 J(p)}{\partial p_1 \partial p_2} & \frac{\partial^2 J(p)}{\partial p_2^2} & \frac{\partial^2 J(p)}{\partial p_2 \partial p_3} & \frac{\partial^2 J(p)}{\partial p_2 \partial p_4} \\ \frac{\partial^2 J(p)}{\partial p_1 \partial p_3} & \frac{\partial^2 J(p)}{\partial p_2 \partial p_3} & \frac{\partial^2 J(p)}{\partial p_3^2} & \frac{\partial^2 J(p)}{\partial p_3 \partial p_4} \\ \frac{\partial^2 J(p)}{\partial p_1 \partial p_4} & \frac{\partial^2 J(p)}{\partial p_2 \partial p_4} & \frac{\partial^2 J(p)}{\partial p_3 \partial p_4} & \frac{\partial^2 J(p)}{\partial p_4^2} \end{pmatrix}.$$

The components are approximated by

$$\frac{\partial^2 J(p)}{\partial p_i \partial p_j} \approx \frac{1}{4h^2}\big(J(p+h(e_i+e_j)) - J(p-h(e_i-e_j))$$
$$-J(p+h(e_i-e_j)) + J(p-h(e_i+e_j))\big),\quad i,j=1,\ldots,4,$$

where e_i and e_j are the i-th and j-th unit vector, respectively. For the particular case $i=j$ this formula reduces to

$$\frac{\partial^2 J(p)}{\partial p_i^2} \approx \frac{J(p+2he_i) - 2J(p) + J(p-2he_i)}{4h^2},\qquad i=1,\ldots,4.$$

The gradient of the cost function

$$\nabla J(p)=\left(\frac{\partial J}{\partial p_1},\frac{\partial J}{\partial p_2},\frac{\partial J}{\partial p_3},\frac{\partial J}{\partial p_4}\right)(p)$$

is approximated by central finite differences:

$$\frac{\partial J}{\partial p_j}(p) \approx \frac{J(p+he_j)-J(p-he_j)}{2h},\ j=1,\ldots,4,$$

where e_j is the *j*-th unit vector and *h* is a small value, that is recommended to be the cubic root of the machine accuracy. With respect to the parametrization of the governing equation we set

$$p_1 = C,\qquad p_2=\sigma_0,\qquad p_3=k,\qquad p_4=\phi_{\mathrm{c}}.$$

3. Results

3.1 Hessian matrix and condition numbers

In Tables 1 and 2 the entries of the Hessian (matrix) in the cost minimum for the simultaneous identification of all four parameters is given for the cases of intermediate and stationary observation profiles, respectively. Here, we refer to a profile as “intermediate” if it is observed at a time when the suspension is still undergoing transient settling and compression, while a profile is called “stationary” if the sediment has already attained the final steady state. The condition numbers of the Hessians are calculated as

$$\kappa(H_i) = 7.7643 \cdot 10^4, \qquad \kappa(H_s) = 1.2847 \cdot 10^8$$

for the intermediate and stationary data, respectively. The intermediate data produce significantly smaller condition number than the stationary. On the other hand, stationary data lead to a stabler algorithm and more reliable estimation, and are therefore clearly preferable for parameter identification.

It can be observed that the entry corresponding to the critical concentration $J_{\phi_c\phi_c}$ is dominant by several orders of magnitude. At the same time, the other parameters correlate negatively with the critical concentration ϕ_c. In comparison, the matrix related to the stationary profile shows greater entries than that related to the intermediate profile. In the latter case there is the inconvenience that $J_{CC} < 0$, which means that according to numerical accuracy there is not a local minimum and thus numerical identification is endangered to fail. Observing the diagonals of the Hessians one can judge that the parameter ϕ_c is distinctly most sensitive, followed by σ_0 and then k, whereas the exponent C is the least sensitive.

In Figure 2 the properties of the Hessians in the cost minimum are shown, comparing the cases of observations at intermediate state versus at stationary state. The overall observation is that in the transient regime, and throughout all parameter sets, the condition numbers of the Hessians in the cost minimum are smaller and the distribution of the singular values resulting from a singular value decomposition (SVD) is more equilibrated. This means that the identification for observations at intermediate time is more feasible and promising. We will be specific about this point in the following.

In Figures 2 (a) and (b) the decadic logarithm of the condition numbers of the Hessian in the cost optimum for all parameter sets with two or three parameters are compared. For each possible parameter set, intermediate observations show a smaller condition number than stationary ones. A smaller condition number indicates that the respective parameters are less correlated and show smaller parameter dependence. A smaller condition number means geometrically that the “valley” of the cost function is less deep, and numerically that an approximation of the cost function by a quadratic function is exposed to less numerical errors, making the identification algorithm more stable.

In the case with two parameters one can observe a common structure for both intermediate and stationary observations: for the parameter pair (σ_0, ϕ_c) the largest condition number is obtained, and for (C, σ_0) the smallest. This means that the parameter σ_0 is present in both extremes, even though it can be judged (by the diagonal of the Hessian) to be third most sensitive, and is thus not expected to be present in the case of largest condition number.

In both types of observation, the parameter ϕ_c is present in the cases of three highest sensitivities, and C appears in the cases of the two lowest sensitivities, confirming the conjectures derived from the cases of one single parameter. For the stationary profile, the parameter k correlates less than C with ϕ_c, reversing the situation of the intermediate profile.

In a similar way, the parameter pair (σ_0, k) has less sensitivity than (C, k) for stationary observations, while the reverse holds for the intermediate profile. In both cases, the "hyperbolic" parameter C contributes to relatively small sensitivity in the transient case and to relatively large sensitivity for the stationary case. This corresponds to the expectation that a parameter related to the convective term provides a better performance if identified at intermediate state since the convective term is active in non-stationary profiles only.

In Figure 2 (b) the condition numbers of all Hessians in the cost minimum depending on three parameters are shown. The previous observations can be confirmed: the intermediate profile always leads to better condition numbers than the stationary profile. The parameter set (C, σ_0, k) (without the critical concentration ϕ_c) clearly shows less dependence within the parameter set than the parameter sets including ϕ_c. It can be noted that the condition number of the set (C, σ_0, k) for the end profile has the same order of magnitude as the sets with the sensitive parameter ϕ_c in the intermediate profile. Roughly speaking, here, a bad parameter choice at good observation conditions is equivalent to a good parameter choice at bad conditions. It is remarkable that the parameter choice (σ_0, k, ϕ_c), which excludes the convective parameter C, at the end profile is more strongly correlated than the other choices where both the critical concentration ϕ_c and the parameter C are included. This means that the parameter C representing the convection term has a stabilizing effect. Most interestingly, this clearly stronger correlation in the set of diffusion parameters (σ_0, k, ϕ_c) cannot be observed in the case of a transient observation profile.

In Figure 2 (c) the singular values are plotted for each parameter set containing three parameters. In both cases of intermediate and stationary profile observations, for the parameter set (C, σ, k) the largest singular values are smaller than in the other cases obtained from the same type of observation. In the case of stationary profiles all parameters sets yield similar largest singular values. For the parameter set (σ_0, k, ϕ_c), the smallest singular value is clearly smaller than in the other cases, which explains the exceptionally bad condition number.

In Figure 2 (d) the singular values are shown for the Hessian matrix in the cost minimum for the complete set containing all four parameters. One can observe the dominance of the largest singular value, which could be anticipated by the singular dominance of $J_{\phi_c \phi_c}$ in the Hessian. For the case with a stationary observation profile, the smallest singular value is clearly smaller than the other singular values, which is not the case of intermediate observation data. By the observations on the parameter set (σ_0, k, ϕ_c), which have a remarkable worse condition for stationary data, the lower smallest singular value for the complete parameter set in the stationary data case can be associated to the strong redundancy of the diffusion parameter.

3.2 Cost function

In Figures 3 and 4, the one-parameter cost functions for both intermediate and stationary observation profiles near the cost optimum, respectively, are plotted. While close to the cost minimum, convexity can be confirmed in all cases, anomalies far from the cost minimum can be observed in several occasions:

- For the parameter k in the intermediate case, the cost function flattens for small values and it shows several inflection points for values to the right of the minimum. This behaviour causes the difficulty or even impossibility to apply gradient methods at least when the initial guess is chosen far from the optimum (see Figure 3(c)).
- For the parameter k in the stationary case there are several non-smooth points, one directly in the minimum and one close to the parameter value 9,15. This non-smoothness makes the algorithm to work inefficiently (Figure 4(c)).

- For the parameter C in the case of stationary observation data the cost function asymmetrically increases on the two sides of the minimum. While there is a strong increase to the right hand side, there is only a slight increase on the left side. Numerical experiments show that when the initial guess is chosen on the right side, then there is a rapid convergence whereas with data from the left side the convergence get slow or even might fail, in particular due to the a local minimum close to 2,75. See Figure 4 (a).
- For the parameter ϕ_c in the stationary case there are several regions of non-convexity and points of discontinuity (see Figure 4(d)).

In conclusion, this non-convexity and non-smoothness of the cost function lets the gradient algorithm work very slowly or even fail. Things get even more complicated for two-parameter sets by combining anomalies of two parameters.

Figures 5 and 6 show the cost function of all possible two-parameter sets related to intermediate and stationary observation profile, respectively. The graphics extend the quantitative results obtained by the evaluation of the condition numbers of the Hessian matrix and the qualitative observations based on the cost function plots of the one-parameter sets.

In Table 5 the qualitative behaviour for parameter sets with two parameters is enlisted. The qualitative behaviour is obtained by visual inspection, where saddle-point behaviour and regions of non-convexity have been detected. (We refer to *saddle-point behaviour* if there are points where the second derivatives with respect to one parameter have different signs, while *non-convexity* means inflection points of the cost function, where it switches from a convex to concave shape.) The non-convexity of the cost functions results in an over- or underestimation of the scale, whereas a saddle-point tendency can lead to wrong directions. Both phenomena counteract the assumption of convexity which is a basic hypothesis to ensure an appropriate performance of gradient methods.

To illustrate these phenomena, take the cost plot of the parameter set (C, ϕ_c) for the intermediate observations (Figure 5(c)). While close to the cost minimum one can detect convexity of the cost function, convexity fails away from the cost minimum. Taking an initial parameter guess at e.g. $(C, \phi_c) = (5, 0.14)$ then the gradient points due to a local saddle point structure in a completely other direction than towards the cost minimum. Taking an initial guess at $(C,\phi_c)=(2,0.14)$ then the gradient direction appears more appropriate but the slope yields a clear underestimation.

In Table 6 identification runs for each two-parameter set are reported. The goal is to examine the performance of the identification algorithm depending on the parameter choice. For each parameter set two runs with different initial guesses far from the optimal parameter are performed, in each case with both intermediate and stationary observation profiles. This means that the success of the identification algorithm basically depends on the considered observation profile and the chosen initial guess. The identification is stopped either if the convergence criterion is met, i.e. if the gradient norm is below a tolerance value, or after 200 iteration as upper limit. The identified parameter set $p^{(n)}$ is reported together with the calculated cost inimum $J\left(p^{(n)}\right)$ and the condition number of the Hessian matrix in that parameter set, $\kappa\left(H\left(p^{(n)}\right)\right)$.

Clearly, one can enforce convergence by choosing the initial guess close enough to the optimal parameter. In the case that the optimal parameter is not known a pragmatic approach is to try several initial guesses. Then by chance one makes a choice close to the optimum or opportune convergence behaviour beeing on the more convex side. The goal of the present test runs is just to document the bad convergence behaviour without applying such pramgamtic strategies.

Heuristically, from Table 6 we have that the best value for $d\left(p,p^{(n)}\right)$ is of the order of magnitude 10^{-5} and the best value for $J\left(p^{(n)}\right)$ is around $4\cdot 10^{-12}$. In the sequel the observations are detailed.

For the parameter set (σ_0,ϕ_c) a rapid decrease of the cost function is observed identifying very well one parameter, namely (σ_0,ϕ_c). However, the other parameter remains far from its optimum with the consequence that the approximated parameter pair remains far from its optimum. This biased identification behaviour can be explained by the fact that the condition number of the Hessian is above the square root of the machine error. Another observation for this parameter pair is that very similar parameter approximations are obtained for both observation profile types.

For the parameter pair (k, ϕ_c) a perfect performance in case 5 (with an intermediate observation profile) is observed, whereas very slow performance in the other cases (6,7,8) leading to parameters far from the optimum.

For the parameters (C, ϕ_c) a very good performance in cases 9 and 11 is observed, where an intermediate observation profile is used. The test case 10 is very interesting, since there is a poor condition number, which is above the square root of the machine accuracy (order of magnitude 10^{-8}). The square root of the machine error is the threshold value above of which numerical errors are expected to eliminate the number of significant digits. In test run 10 there is convergence even though the distance $d\left(p, p^{(n)}\right)$ and the cost function $J\left(p^{(n)}\right)$ underperform the optimal benchmark values just in the order of magnitude of the difference of the condition number of the Hessian matrix to the square root of machine accuracy.

The test runs with the parameter set (σ_0, k) are somehow surprising, since in the cases 13 and 15 there is a very small condition number, but the identification is stopped by meeting the maximum number of allowed iterations with a result very far away. It is assumed that the gradient points towards a completely wrong direction. Case 16 is also remarkable since there is a very good performance of the identification with stationary data while the identification of the same data with intermediate observation fails.

For parameter pair (C, k), the case 17 with intermediate profile gives an excellent result whereas the corresponding case 18, with stationary data, converges only slowly. Case 20 with stationary data gives not an excellent but a reasonable result. The corresponding case 19 with intermediate profile works very slowly. This means, stationary profiles are in general able to outperform intermediate observation profiles.

For the parameter set (C, σ_0) in cases 22 and 23 there appears again the wrong-direction phenomenon: Even though the condition number is very promising, the algorithm is stopped by reaching the maximum number of iterations. Case 24 is somehow particular since the run is stopped after only 4 iterations being on the right way but not far enough. The reason of the early stop is the small gradient of the cost function.

In conclusion, for the intermediate profile the algorithm works well in most of the cases. One could expect this, since in such profile, there is more information in the direct problem.

However, the initial guess is crucial for an appropriate performance of the identification task. When the stationary observation profile is used then generally a very slow convergence of the optimization algorithm is encountered. This reflects the observation on basis of the evaluation of the Hessian matrix. Also the graphics of the cost function contribute to understand the behaviour of the identification algorithm when we try to identify one or two parameters.

In Figure 7 the evolution of the cost function during the identification process is shown.

4. Conclusions

Several previous studies on parameter identification for flocculated suspensions at several revealed the ill-posedness of the problem (Berres et al. [26,27], Coronel et al. [33]). In this work the convergence behaviour of the identification procedure has been evaluated quantitatively. In particular, the two cases of observation data given by either intermediate (transient) or stationary profiles are considered and compared. As a central result from the analysis of the corresponding Hessians we conclude that the intermediate (transient) data allow a significantly more robust, and therefore more reliable, identification of parameters than stationary data.

In previous studies it was detected that the critical concentration ϕ_c plays a crucial role in the ill-posedness of the overall identification, but this observation had never been pursued further. Here, parameter sets that either include or exclude ϕ_c are evaluated.

As a surprising result, the identification parameter set containing all three parameters that determine the effective solid stress function $\sigma_e(\phi)$ produces for stationary data an identification of remarkably inferior quality than in other cases that include ϕ_c. This is surprising since in the case of intermediate profile the set of the three diffusive parameters does not behave so badly even though then the parabolic parameters do not play an active role.

The ill-posedness far from the cost minimum is illustrated qualitatively by the plots of the cost functions both for one-parameter and two-parameter sets. There one can observe non-convexity in various instances like convex-concave regions and saddle-point structure by negative combined second derivatives. This non-convexity contradicts all assumptions on gradient methods like the cg or the Quasi-Newton method, which ideally intend an approximation by a quadratic positive definite function.

A series of identifications has been performed with varying parameter sets and initial guesses far from the cost minimum. Several parameter choices which provide a very slow or no convergence are detected and this inconvenient behaviour is documented together with the condition number of the corresponding Hessian. By these test identifications the feasibility of the parameter identification in dependence of the choice of the parameter sets indicated by the study before is confirmed.

Acknowledgements

SB and RG acknowledge support by Conicyt (Chile) through Fondecyt project 11080253. RB and RG acknowledge support by Conicyt (Chile) through Fondecyt project 1090456. In addition, RB acknowledges support by Fondap in Applied Mathematics, project 15000001, and BASAL project CMM, Universidad de Chile and Centro de Investigación en Ingeniería Matemática (CI^{2}MA), Universidad de Concepción, and project AMIRA P996/INNOVA 08CM01-17 “Instrumentación y Control de Espesadores”.

References

1. Bürger, R.; Concha, F. Settling velocities of particulate systems: 12. Batch centrifugation of flocculated suspensions. International Journal of Mineral Processing **2001,** *63*, 115–145.
2. Berres, S.; Bürger, R. On gravity and centrifugal settling of polydisperse suspensions forming compressible sediments. International Journal of Solids and Structures **2003**, *40*, 4965–4987.
3. Garrido, P.; Concha, F.; Bürger, R. Settling velocities of particulate systems: 14. Unified model of sedimentation, centrifugation and filtration of flocculated suspensions. International Journal of Mineral Processing **2003**, *72*, 57–74.
4. Berres, S.; Bürger, R.; Karlsen, K.H.; Tory, E.M. Strongly degenerate parabolic-hyperbolic systems modeling polydisperse sedimentation with compression. SIAM Journal on Applied Mathematics **2003**, *64*, 41–80.
5. Anestis, G.; Schneider, W. Application of the theory of kinematic waves to the centrifugation of suspensions. Ingenieur-Archiv **1983**, *53*, 399–407.

6. Bürger, R.; García, A. Centrifugal settling of polydisperse suspensions with a continuous particle size distribution: a generalized kinetic description. Drying Technology **2008**, *26*, 1024–1034.
7. Detloff, T.; Lerche, D. Centrifugal separation in tube and disc geometries: experiments and theoretical models. Acta Mechanica **2008**, *201*, 83–94.
8. Lerche, D.; Frömer, D. Theoretical and experimental analysis of the sedimentation kinetics of concentrated red cell suspensions in a centrifugal field: Determination of the aggregation and deformation of RBC by flux density and viscosity functions. Biorheology **2001**, *38*, 249–262.
9. Lueptow, R.M.; Hübler, W. Sedimentation of a suspension in a centrifugal field. Journal of Biomechanical Engineering **1991,** *113*, 485–491.
10. Biesheuvel, P.M.; Nijmeijer, A.; Verweij, H. Theory of batchwise centrifugal casting. American Institute of Chemical Engineers Journal **1998**, *44*, 1914–1921.
11. Biesheuvel, P.M.; Verweij, H. Calculation of the composition profile of a functionally graded material produced by centrifugal casting. Journal of the American Ceramic Society **2000**, *83*, 743–749.
12. Sambuichi, M.; Nakakura, H.; Osasa, K.; Tiller, F.M. Theory of batchwise centrifugal filtration. AIChE Journal, **1987**, *33*, 109–120.
13. Demeler, B.; Saber, H.; Hansen, J.C. Identification and interpretation of complexity in sedimentation velocity boundaries. Biophysical Journal **1997**, *72*, 397–407.
14. Stickland, A.D.; White, L.R.; Scales, P.J. Modeling of solid-bowl batch centrifugation of flocculated suspensions. American Institute of Chemical Engineers Journal **2006**, *52*, 1351–1362.
15. Schaflinger, U. Centrifugal separation of a mixture. Fluid Dynamics Research **1990**, *6*, 213–249.
16. Stibi, H.; Schaflinger, U. Centrifugal separation of a mixture in a rotating bucket. Chemical Engineering Science, **1991**, *46*, 2143–2152.
17. Chu, C.P.; Lee, D.J. Dewatering of waste activated sludge via centrifugal field. Drying Technology **2002**, *20*, 953–966.
18. Chu, C.P.; Lee, D.J. Centrifugation of polyelectric flocculated clay slurry. Separation Science and Technology **2002**, *37*, 591–605.

19. Detloff, T.; Sobisch, T.; Lerche, D. Particle size distribution by space or time dependent extinction profiles obtained by analytical ultracentrifugation. Particle & Particle Systems Characterization **2006**, *23*, 184–187.

20. Detloff, T.; Sobisch, T.; Lerche, D. Particle size distribution by space or time dependent extinction profiles obtained by analytical centrifugation (concentrated systems). Powder Technology **2007**, *174*, 50–55.

21. Eckert, W.F.; Masliyah, J.H.; Gray, M.R.; Fedorak, P.M. Prediction of sedimentation and consolidation of fine tails. AIChE Journal **1996**, *42*, 960–972.

22. Frömer, D.; Lerche, D. An experimental approach to the study of the sedimentation of dispersed particles in a centrifugal field. Archive of Applied Mechanics **2002**, *72*, 85–95.

23. Hwang, K.-J.; Chou, K.-H. Effect of cake compression on the performance of centrifugal dewatering. Drying Technology **2006**, *24*, 1263–1270.

24. Lerche, D. Dispersion stability and particle characterization by sedimentation kinetics in a centrifugal field. Journal of Dispersion Science and Technology **2002**, *23*, 699–709.

25. Sambuichi, M.; Nakakura, H.; Osasa, K. Zone settling of concentrated slurries in a centrifugal field. Journal of Chemical Engineering of Japan **1991**, *24*, 489–494.

26. Berres, S.; Bürger, R.; Coronel, A.; Sepúlveda, M. Numerical identification of parameters for a strongly degenerate convection-diffusion problem modelling centrifugation of flocculated suspensions. Applied Numerical Mathematics **2005**, *52*, 311–337.

27. Berres, S.; Bürger, R.; Coronel, A.; Sepúlveda, M. Numerical identification of parameters for a flocculated suspension from concentration measurements during batch centrifugation. Chemical Engineering Journal **2005**, *111*, 91–103.

28. Kada, B.; Tarasiewicz, S. Analysis and identification of distributed parameter model for wood drying systems. Drying Technology **2004**, *22*, 933–946.

29. Weres, J.; Olek, W.; Guzenda, R. Identification of mathematical model coefficients in the analysis of the heat and mass transport in wood. Drying Technology, **2000**, *18*, 1697–1708.

30. Richardson, J.F.; Zaki, W.N. Sedimentation and fluidization: Part I. Transcations of the Institution of Chemical Engineers (London) **1954**, *32*, 35–53.

31. Tiller, F.M.; Leu, W.F. Basic data fitting in filtration. Journal of the Chinese Institution of Chemical Engineers **1980**, *11*, 61–70.

32. Engquist, B.; Osher, S. One-sided difference approximations for non-linear conservation laws. Mathematics of Computation **1981**, *36*, 321–351.
33. Coronel, A.; James, F.; Sepúlveda, M. Numerical identification of parameters for a model of sedimentation processes. Inverse Problems **2003**, *19*, 951–972.

List of table captions

Table 1: Hessian matrix in the cost minimum corresponding to identification with observations given by the intermediate observation profile.

Table 2: Hessian matrix in the cost minimum corresponding to identification with observations given by the stationary observation profile.

Table 3: Tabular listing of the values in Figure 2 (a), condition numbers for parameter sets with two parameters.

Table 4: Tabular form of Figure 2 (b), condition numbers for parameter sets with three parameters.

Table 5: Qualitative behaviour for parameter sets with two parameters, detecting saddle-point behaviour and one-directional non-convexity

Table 6: Identification runs for two-parameter sets. The identified parameter pairs (IP) are referred to by capital letters: A: (σ_0, ϕ_c), B: (k, ϕ_c), C: (C, ϕ_c), D: (σ_0, k), E: (C, k), F: (C, σ_0). The type of observation profile (PT) is either "intermediate" (i) or "stationary" (s). Moreover, we display the optimal parameter (OP) and the initial guess (IG), the number of iterations n to meet the convergence criterion (with 200 iteration as upper limit), the identified parameter set $p^{(n)}$, the calculated cost minimum $J\left(p^{(n)}\right)$ in the identified parameter set, the distance between the identified parameter $p^{(n)}$ and the optimal

parameter p, and the condition number of the Hessian of the cost function evaluated at the identified parameter, $\kappa^{(n)} = \kappa\left(H\left(p^{(n)}\right)\right)$.

List of figure captions

Figure 1: (a) Evolution of the solution of the direct problem in space and time, (b) numerical approximation of intermediate and final profiles

Figure 2: Evaluation of Hessian matrices, stationary profile (solid line) and intermediate profile (dashed line)

(a) Log10 of the condition number of the Hessian matrix in the cost minimum for all parameter sets with 2 parameters
(b) Log10 of the condition number of the Hessian matrix in the cost minimum for all parameter sets with 3 parameters
(c) Log10 of the singular values of the Hessian matrix in the cost minimum for all parameter sets with 3 parameters
(d) Log10 of the singular values of the Hessian matrix in the cost minimum for the parameters set with 4 parameters

Figure 3: One-parameter cost functions for each parameter (a) C, (b) σ_0, (c) k, (d) ϕ_c;, obtained with intermediate observation profiles.

Figure 4: One-parameter cost functions for each parameter (a) C, (b) σ_0, (c) k, (d) ϕ_c, obtained with stationary observation profiles.

Figure 5: Two-parameter cost functions for each parameter set (a) (σ_0, ϕ_c), (b) (k, ϕ_c), (c) (C, ϕ_c), (d) (σ_0, k), (e) (C, k), (f) (C, σ_0) for the intermediate observation profile.

Figure 6: Two-parameter cost functions for each parameter set (a) (σ_0, ϕ_c), (b) (k, ϕ_c), (c) (C, ϕ_c), (d) (σ_0, k), (e) (C, k), (f) (C, σ_0) for the stationary observation profile.

Figure 7: Evolution of the cost function during the identification process. The symbols are related to the test cases and parameter sets in Table 6 as follows:

(a) (σ_0, ϕ_c): 1 '×', 2 '∘', 3 '*', 4 '+',

(b) (k, ϕ_c): 5 '×', 6 '∘', 7 '*', 8 '+',

(c) (C, ϕ_c): 9 '×', 10 '∘', 11 '*', 12 '+',

(d) (σ_0, k): 13 '×', 14 '∘', 15 '*', 16 '+',

(e) (C, k): 17 '×', 18 '∘', 19 '*', 20 '+',

(f) (C, σ_0): 21 '×', 22 '∘', 23 '*', 24 '+',

Table 1:

	C	σ_0	k	ϕ_c
c	-0.0006	0.0002	0.0015	-0.0869
k	0.0002	0.0006	0.0010	-0.0637
σ	0.0015	0.0010	0.0084	-0.3975
ϕ_c	-0.0869	-0.0637	-0.3975	20.2158

Table 2:

	C	σ_0	k	ϕ_c
c	0.00003	0.000030	0.00247	-0.18481
k	0.00030	0.004236	0.00320	-0.21729
σ	0.00247	0.032020	0.24221	-16.427
ϕ_c	-0.18481	-0.21729	-16.427	1114.76

Table 3:

	(σ_0,ϕ_c)	(k,ϕ_c)	(C,ϕ_c)	(σ_0,k)	(C,k)	(C,σ_0)
Intermediate	5.7803e+4	3.3393e+4	1.9827e+4	20.6688	9.6725	1.1664
Stationary	3.262e+10	7.8652e+6	2.0188e+8	1.1019e+5	4.4996e+4	7.8286e+2

Table 4:

	(σ_0,k,ϕ_c)	(C,σ_0,ϕ_c)	(C,k,ϕ_c)	(C,σ_0,k)
Intermediate	8.5909e+4	5.6555e+4	3.2578e+4	21.2850
Stationary	1.7380e+10	1.7723e+7	5.8435e+6	8.3379e+3

Table 5:

	(σ_0,ϕ_c)	(k,ϕ_c)	(C,ϕ_c)	(σ_0,k)	(C,k)	(C,σ_0)
Intermediate		NC	SP	SP		
Stationary	NC, SP	NC	NC	NC, SP		SP

Table 6:

#	IP	PT	OP	IG	n	$p^{(n)}$	$d^{(n)}$	$J^{(n)}$	$\kappa^{(n)}$
1	A	i	(5.7, 9.0)	(3.0, 0.08)	7	(2.998083, 0.093110)	2.70020	9.42e-12	8.53e+9
2	A	s	(5.7, 9.0)	(3.0, 0.08)	7	(2.999811, 0.093116)	2.70193	6.85e-12	2.50e+9
3	A	i	(5.7, 9.0)	(9.0, 0.09)	7	(8.999604, 0.105206)	3.29961	1.27e-11	3.75e+10
4	A	s	(5.7, 9.0)	(9.0, 0.09)	9	(8.996619, 0.105202)	3.29662	2.34e-11	2.43e+10
5	B	i	(9.0, 0.1)	(4.0, 0.05)	92	(9.001084, 0.100014)	0.00108	1.97e-11	3.61e+6
6	B	s	(9.0, 0.1)	(4.0, 0.05)	134	(8.320567, 0.089742)	0.67951	3.81e-5	5.52e+6
7	B	i	(9.0, 0.1)	(13.0, 0.1)	39	(12.998922, 0.144271)	3.99917	8.10e-5	4.24e+8
8	B	s	(9.0, 0.1)	(13.0, 0.1)	146	(9.159601, 0.102344)	0.15962	1.73e-6	7.72e+6
9	C	i	(5.0, 0.1)	(8.0, 0.08)	85	(5.000013, 0.100000)	0.00001	4.14e-12	1.00e+5
10	C	s	(5.0, 0.1)	(8.0, 0.08)	59	(5.094198, 0.100016)	0.09420	9.44e-10	4.74e+9
11	C	i	(5.0, 0.1)	(1.0, 0.16)	68	(5.000011, 0.100000)	0.00001	4.13e-12	1.00e+5
12	C	s	(5.0, 0.1)	(1.0, 0.16)	200	(1.105115, 0.100540)	3.89488	6.13e-5	3.83e+7
13	D	i	(5.7, 9.0)	(10.0, 3.0)	200	(10.005910, 3.088607)	7.31337	4.91e-2	2.25e+2
14	D	s	(5.7, 9.0)	(10.0, 3.0)	153	(7.576703, 8.785610)	1.88891	3.40e-6	1.15e+6
15	D	i	(5.7, 9.0)	(2.0, 4.0)	200	(2.026522, 4.081059)	6.13925	4.91e-2	1.15e+1
16	D	s	(5.7, 9.0)	(2.0, 4.0)	132	(5.698588, 9.000187)	0.00142	2.85e-12	1.11e+5
17	E	i	(5.0, 9.0)	(2.0, 5.0)	29	(5.000019, 9.000003)	0.00002	4.10e-12	1.85e+1
18	E	s	(5.0, 9.0)	(2.0, 5.0)	34	(4.032888, 9.007366)	0.96714	5.77e-8	1.98e+5
19	E	i	(5.0, 9.0)	(9.0, 12.0)	198	(7.442325, 9.332551)	2.90194	2.14e-3	8.19e+0
20	E	s	(5.0, 9.0)	(9.0, 12.0)	86	(4.841348, 9.001659)	0.15866	2.66e-9	1.68e+3
21	F	i	(5.0, 5.7)	(2.0, 9.0)	21	(5.000020, 5.700032)	0.00004	4.09e-12	7.04e+0
22	F	s	(5.0, 5.7)	(2.0, 9.0)	200	(2.046095, 7.927256)	3.69949	4.63e-3	2.96e+0
23	F	i	(5.0, 5.7)	(8.0, 7.0)	200	(5.394523, 7.204722)	1.55558	1.77e-4	1.62e+1
24	F	s	(5.0, 5.7)	(8.0, 7.0)	4	(7.866712, 5.249234)	2.90194	2.97e-5	1.66e+2

Figure 1

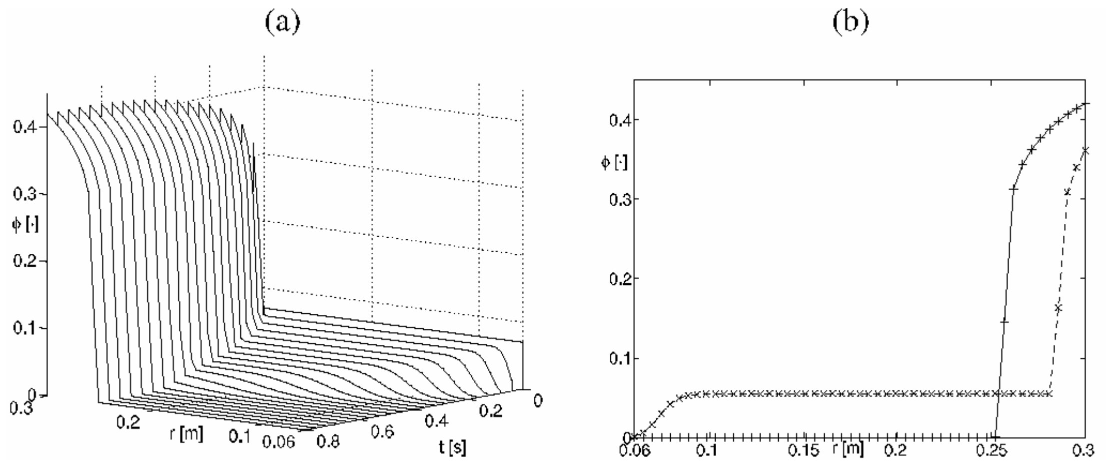

Figure 2

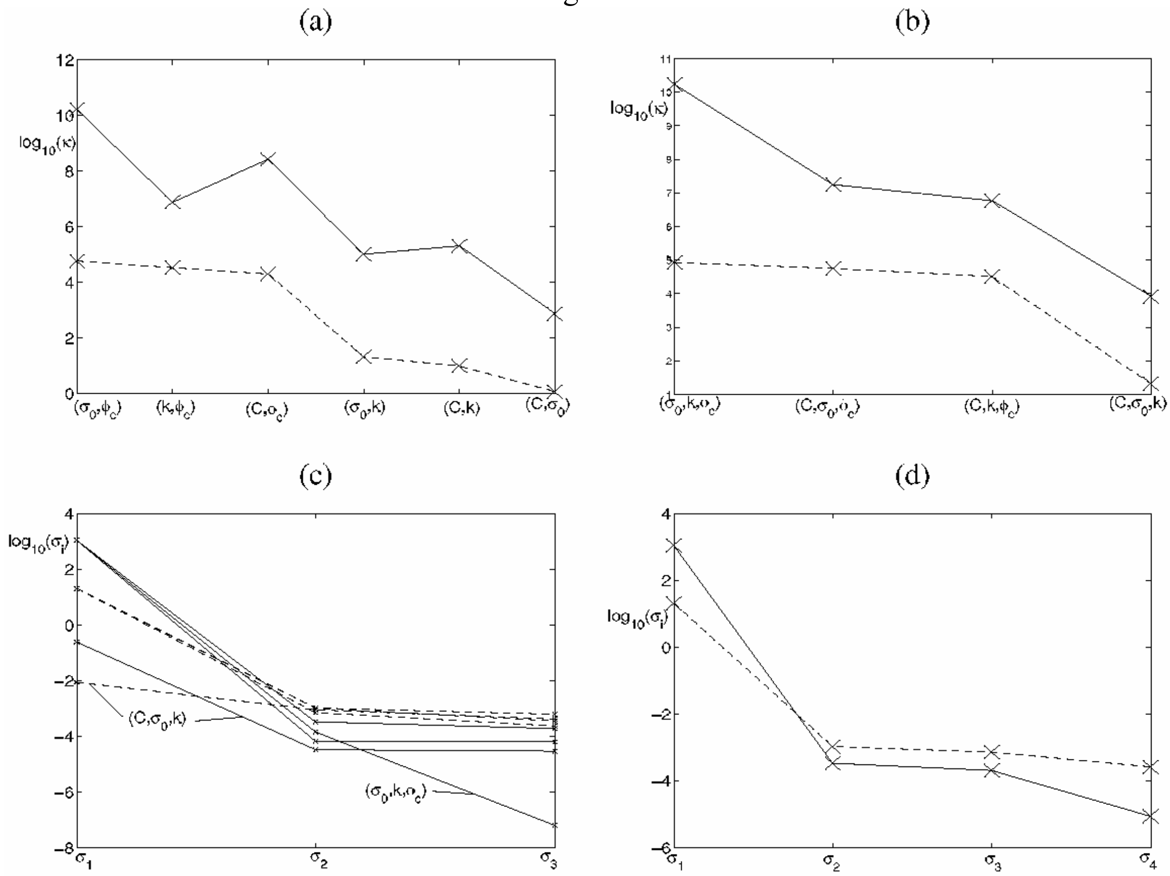

Figure 3

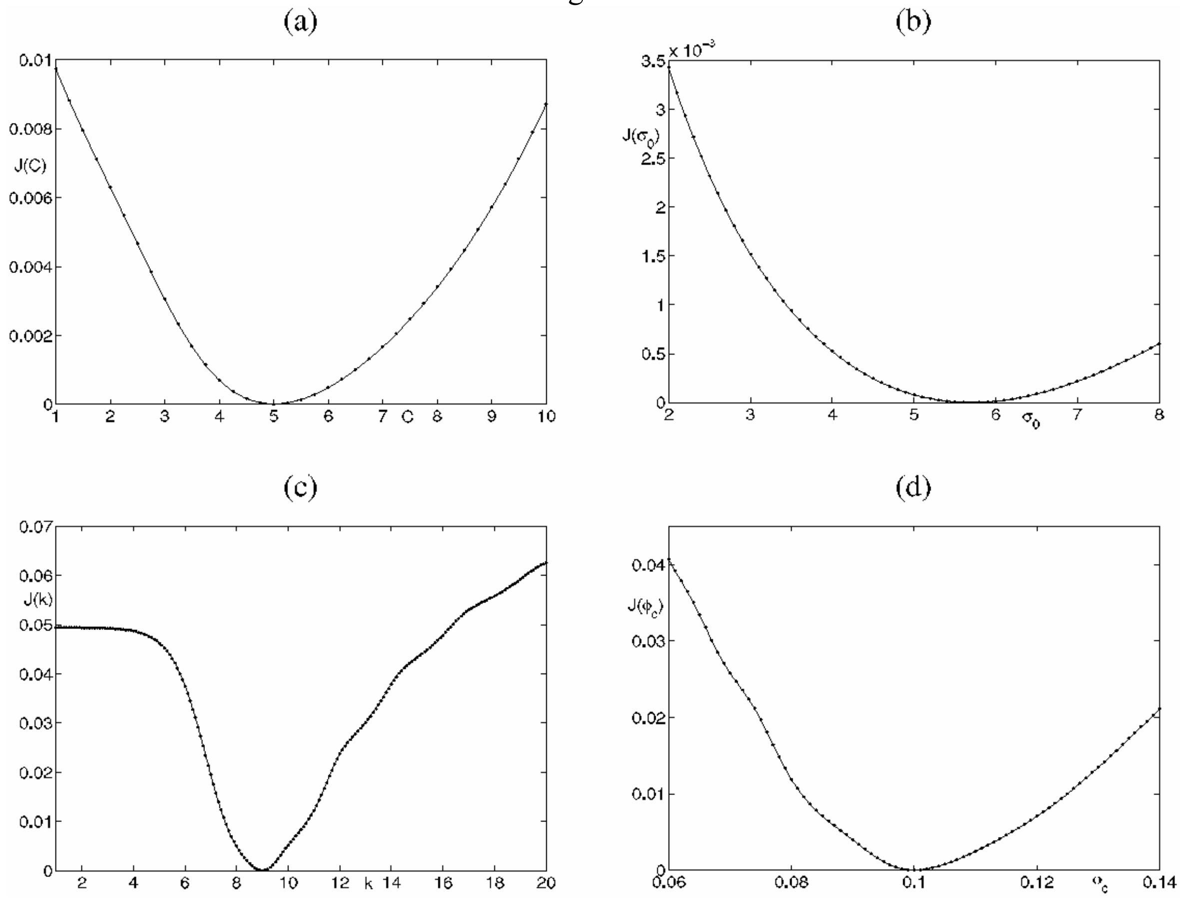

Figure 4

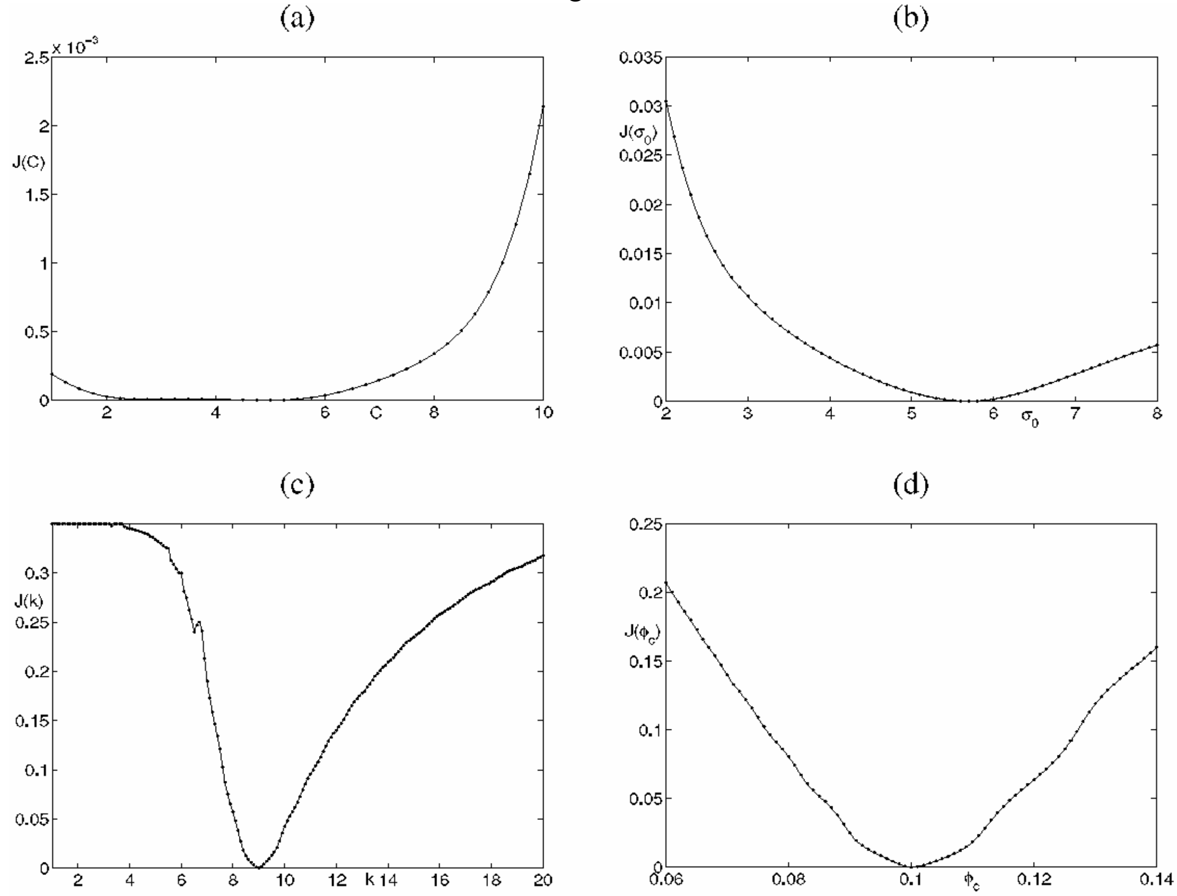

Figure 5

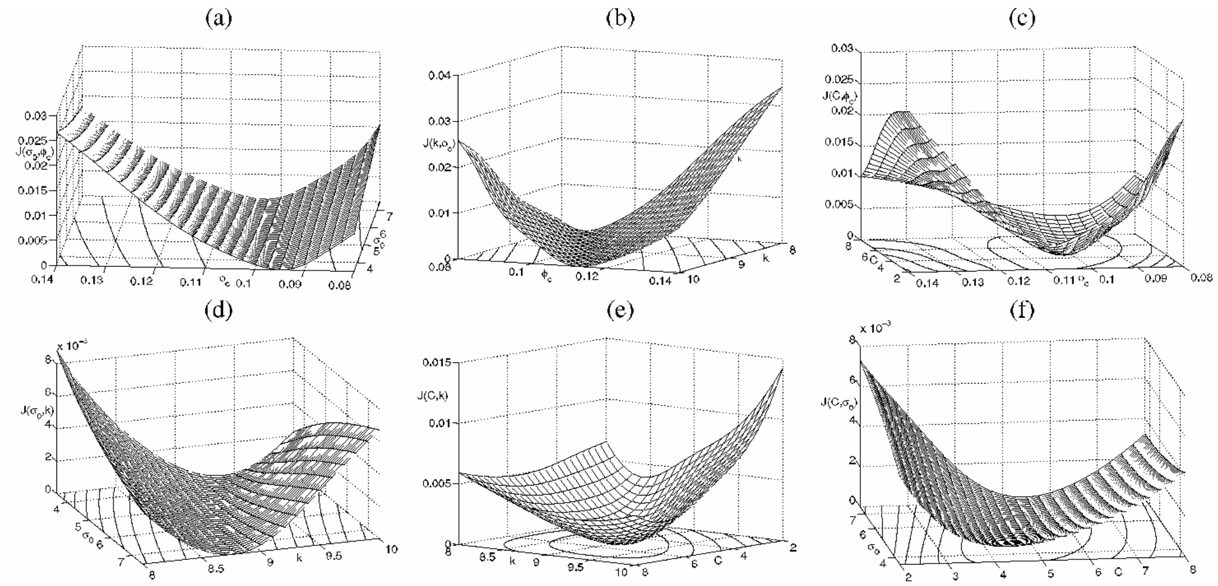

Figure 6

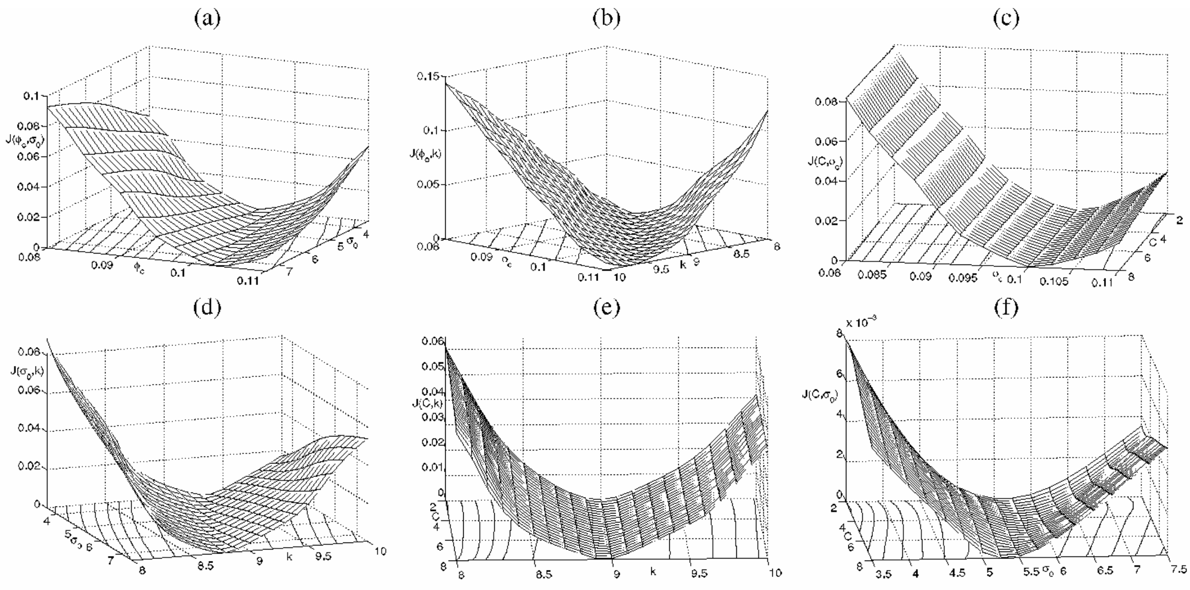

Figure 7

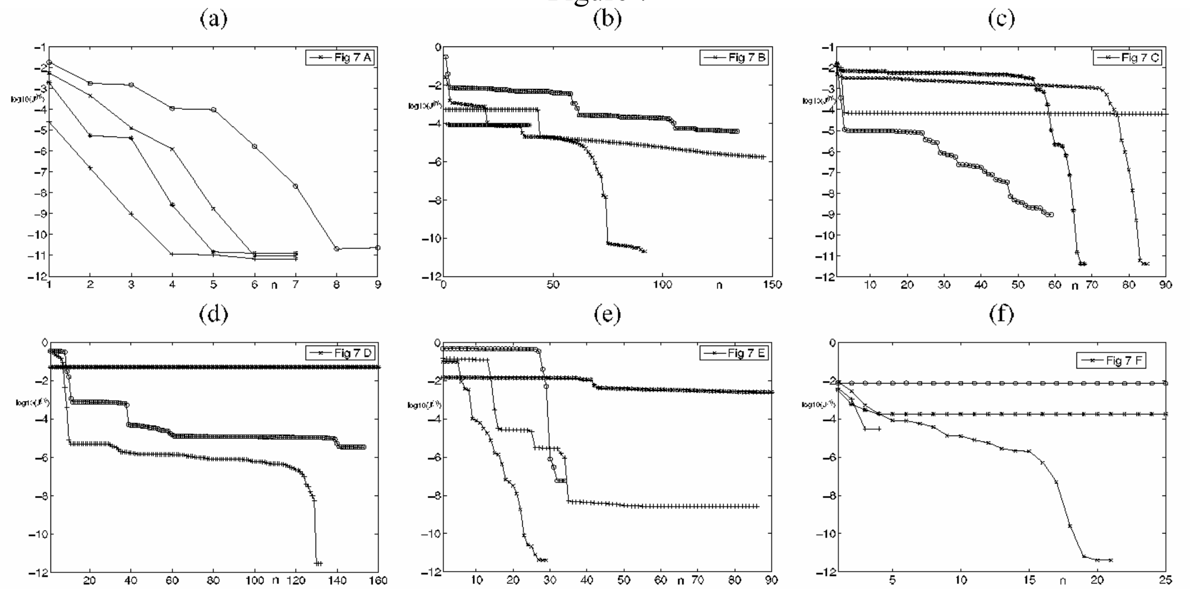

Centro de Investigación en Ingeniería Matemática (CI^{2}MA)

PRE-PUBLICACIONES 2009 - 2010

2009-13 Ricardo Durán, Rodolfo Rodríguez, Frank Sanhueza: *Computation of the vibration modes of a Reissner-Mindlin laminated plate*

2009-14 Gabriel N. Gatica, Antonio Marquez, Manuel A. Sanchez: *Analysis of a velocity-pressure-pseudostress formulation for the stationary Stokes equations*

2009-15 Raimund Bürger, Kenneth H. KARLSEN, John D. Towers: *On some difference schemes and entropy conditions for a class of multi-species kinematic flow models with discontinuous flux*

2009-16 Gabriel N. Gatica, George C. Hsiao, Francisco J. Sayas: *Relaxing the hypotheses of the Bielak-MacCamy BEM-FEM coupling*

2009-17 Iuliu S. Pop, Florin A. Radu, Mauricio Sepúlveda, Octavio Vera: *Error estimates for the finite volume discretization for the porous medium equation*

2009-18 Raimund Bürger, Kenneth H. KARLSEN, Hector Torres, John D. Towers: *Second-order schemes for conservation laws with discontinuous flux modelling clarifier-thickener units*

2009-19 Maria G. Armentano, Claudio Padra, Rodolfo Rodríguez, Mario Scheble: *An hp finite element adaptive scheme to solve the Laplace model for fluid-solid vibrations*

2009-21 Carlos D. Acosta, Raimund Bürger, Carlos E. Mejia: *Monotone difference schemes stabilized by discrete mollification for strongly degenerate parabolic equations*

2009-22 Gabriel N. Gatica, Salim Meddahi: *Finite element analysis of a time harmonic Maxwell problem with an impedance boundary condition*

2009-23 Veronica Anaya, Mostafa Bendahmane, Mauricio Sepúlveda: *Mathematical and numerical analysis for predator-prey system in a polluted environment*

2009-24 Julio Aracena, Eric Fanchon, Marco Montalva, Mathilde Noual: *Combinatorics on update digraphs of discrete networks*

2010-01 Stefan Berres, Raimund Bürger, Rodrigo Garces: *Centrifugal settling of flocculated suspensions: A sensitivity analysis of parametric model functions*

Para obtener copias de las Pre-Publicaciones, escribir o llamar a: Director, Centro de Investigación en Ingeniería Matemática, Universidad de Concepción, Casilla 160-C, Concepción, Chile, Tel.: 41-2661324, o bien, visitar la página web del centro: `http://www.ci2ma.udec.cl`

Centro de Investigación en
Ingeniería Matemática (CI^{2}MA)
Universidad de Concepción

Casilla 160-C, Concepción, Chile
Tel.: 56-41-2661324/2661554/2661316
http://www.ci2ma.udec.cl